Journal of Alloys and Compounds 517 (2012) 157–163

Contents lists available at SciVerse ScienceDirect

Journal of Alloys and Compounds

journal homepage: www.elsevier.com/locate/jallcom

Sol–gel zirconia nanopowders with α-cyclodextrin as organic additive

M. Răileanu[a,*], L. Todan[a,*], D. Crişan[a], N. Drăgan[a], M. Crişan[a], C. Stan[a], C. Andronescu[a], M. Voicescu[a], B.S. Vasile[b], A. Ianculescu[b]

[a] "Ilie Murgulescu" Institute of Physical Chemistry, Roumanian Academy, Splaiul Independenței 202, 060021 Bucharest, Romania
[b] Department of Oxide Materials Science and Engineering, "Politehnica" University of Bucharest, 1-7 Gh. Polizu, P.O. Box 12-134, 011061 Bucharest, Romania

ARTICLE INFO

Article history:
Received 26 July 2011
Received in revised form
13 December 2011
Accepted 15 December 2011
Available online 24 December 2011

Keywords:
Oxide materials
Sol–gel process
Thermal analysis
Scanning electron microscopy
Transmission electron microscopy
X-ray diffraction

ABSTRACT

Nanomaterials present unique structural and physicochemical properties due to their ultra fine size of particles that make them very useful in many domains. The most spectacular applications of nano-sized zirconia include ceramics, piezoelectrics, refractories, pigments, solid electrolytes, oxygen sensors, catalysts, ultrafiltration membranes, and chromatography packing materials. Nanostructured zirconia powders can be prepared using various methods, such as sol–gel process, coprecipitation, hydrothermal synthesis, and reverse micelle method. The aim of the present work was to prepare zirconia nanopowders through the sol–gel method, using α-cyclodextrin as organic additive and to establish its influence on the structural and textural properties of the obtained product. A white, amorphous ZrO_2 powder containing α-cyclodextrin was prepared, which became a crystalline, stable one, after removing the organic matter by thermal treatment. The resulted nanocrystalline powder contains both monoclinic and tetragonal zirconia phases and is very stable. It presents a relatively reduced tendency of agglomeration of particles and contains closed pores which are embedded in the zirconia matrix. The zirconia powders were characterized using the following methods: thermal analysis, IR spectroscopy, UV–vis spectroscopy, X-ray diffraction, and electron microscopy (SEM, TEM, and HRTEM coupled with SAED).

1. Introduction

Zirconia represents one of the most studied oxide materials due to its numerous and important physical and chemical properties, such as high hardness, low thermal conductivity, high melting point, resistance to high temperatures and corrosion, chemical inertness, and amphoteric character [1–3]. Although it has been extensively studied over few decades, the interest of the researchers is still increasing due to the wide range of its applications. The most spectacular ones include ceramics, bioceramics, refractories, piezoelectrics, pigments, cosmetics, solid electrolytes, oxygen sensors, active phases and/or supports in catalysis, column-packing materials for high-performance liquid chromatography (HPLC), and photonics [1,4–13].

Pure zirconia exhibits three polymorphs: low-temperature monoclinic (at $T < 1170\,^{\circ}C$), high-temperature tetragonal (at temperatures between 1170 °C and 2370 °C), and high-temperature cubic (for $T > 2370\,^{\circ}C$). The phase relationship and the structure–property correlation have been very intensively studied [3,9,14–16]. The systems containing ZrO_2 are characterized by phase transformation reactions (of monoclinic polymorphic modification into tetragonal, of tetragonal modification into cubic, and/or by the formation of some intermediate metastable phases during these transformations). The high-temperature polymorphs cannot simply be quenched to room temperature because of their spontaneously martensitic transition to the monoclinic form [3,9,13]. When zirconia is obtained by conventional methods, it is often characterized by a mixture of monoclinic and tetragonal phases which, by coexisting, affect part properties of the product [4,17,18]. The transition between the phases, which implies volume changes, can turn out be highly problematic [16]. In order to avoid this kind of problems, many researchers recommend the doping of ZrO_2 with small quantities of different metal oxides, such as MgO, CaO, Y_2O_3, Gd_2O_3, CeO_2 and Sc_2O_3 [15,16,19–21]. Another way by which the stabilization of the tetragonal and cubic zirconia polymorphs could be obtained is by controlling the size of particles [9]. It is very well known that materials with nanoscale grain sizes present different properties in comparison with themselves in bulk form. They are named "nanostructured materials" and because of their special properties they are intensively studied.

The increasing interest in the nanotechnology of zirconia materials in our days is really remarkable. Many researchers [4,9,14,17,22–24] underlined that, compared to common zirconia powders, the nanocrystalline ones exhibit better physical and chemical properties which lead to wider applications. It is

* Corresponding authors. Tel.: +40 213 167 912; fax: +40 213 121 147.
E-mail addresses: malina_raileanu@yahoo.com (M. Răileanu), ltodan@icf.ro, l_todan@yahoo.co.uk (L. Todan).

0925-8388/$ – see front matter © 2011 Elsevier B.V. All rights reserved.
doi:10.1016/j.jallcom.2011.12.070

considered that all the properties (mechanical, electrical, chemical as well as catalytic) of ZrO_2 can be improved by using nanopowders instead of conventional micron-sized zirconia [23]. In the last decade, the methods of obtaining nanoparticles have significantly developed. They are numerous and include wire explosion techniques, the polymerizable complex method, flame synthesis of nanoparticles, the sonochemical method, solid state reactions, precipitation and co-precipitation from solutions, sol–gel synthesis, forced hydrolysis, microemulsion techniques, microwave-assisted, and hydro- and solvo thermal methods [7,23,25–29].

The selection of the preparation method of nondoped zirconia powders is extremely important, the fact being recognized that the used technique, together with its experimental conditions, significantly influence the characteristics of the final product of the synthesis [4,7,18,30,31]. The sol–gel method represents one of the most popular among those previously mentioned in order to prepare zirconia nanoparticles [10,32–38].

The present work deals with the preparation of a stable, nanocrystalline zirconia powder using the sol–gel approach. In order to confer special properties to the final product, α-cyclodextrin has been used as organic additive. In the last years there are some researchers which studied the synthesis of zirconia powders in the presence of different template agents, especially in order to obtain mesoporous materials. Some examples are: Yu and Hu [22] which used cationic and anionic surfactants (hexadecyltrimethylammonium bromide and sodium dodecyl sulphate, respectively), Suciu et al. [23] that used sucrose and pectin, Ortiz-Landeros et al. [39] which have used polystyrene latex particles, Duan et al. [10] with poly(methyl methacrylate) template, and Heshmatpour and Aghakhanpour [16] with glucose and fructose. The last mentioned researchers [16] suggested that the used organic additives produced some desirable effects on the crystallite size and on the crystal phase of the prepared zirconia powders. Besides these effects, in our study a special powder morphology consisting in embedded pores inside the nanocrystalline ZrO_2 particles was obtained. Only very few researchers such as Chang et al. [26] have reported till now the preparation of porous zirconia crystals. They prepared the material using the combination of sol–gel and hydrothermal methods and they refer to the obtained porous structure as "unique", considering it very important in applications such as thermal barrier coatings (TBCs).

2. Materials and methods

ZrO_2 powder has been synthesized via hydrolysis of zirconium(IV) i-propoxide, i-$Zr(OC_3H_7)_4$ (70 wt.% solution in 1-propanol) from Fluka, in an alcoholic solution of 1-propanol alcohol, C_3H_8O, also from Fluka. The necessary water has been added as aqueous solution of α-cyclodextrin (α-CD), $C_{36}H_{60}O_{30}$, a cyclic oligosaccharide composed of six glucose monomers, from Wacker-Chemie GMBH which has been used as organic additive.

The mixture of the mentioned alcohol and alcoxide in the molar ratio of 7/1 has been maintained under agitation for 15 min (solution 1). An 8 wt.% aqueous solution of α-CD (solution 2) was added drop by drop to solution 1, in a quantity corresponding to the molar ratio H_2O/alcoxide of 18/1, under vigorous stirring. The pH of the reaction mixture was 7. After an induction time of few tens of seconds, a sudden precipitation has been observed. The formation of ZrO_2 particles was evident from the white colour of the precipitate. A very slow stirring has been continued for 2 h, then the static conditions have been maintained for 24 h, in order to ensure the completion of both hydrolysis and condensation reactions. The next step was the drying at 80 °C until the complete removal of the solvent. The obtained material has been crushed in order to obtain the powder which has been named "ZrCD-untt", representing the untreated (before the thermal treatment) zirconia powder containing α-CD. Based on the thermal behaviour of both ZrCD-untt, and α-CD materials, the temperature of the thermal treatment has been chosen, in order to eliminate the organic material from the zirconia powder. The resulted sample was named "ZrCD-tt" (thermally treated).

Both powders have been characterized using the following methods: (1) thermal analysis up to 1000 °C, using a Mettler Toledo Star System TGA/SDTA851/LF 1600 °C, with a heating rate of 10 K min^{-1}, in dynamic air atmosphere, and with a flow of 50 mL min^{-1}; (2) infrared spectroscopy analysis (IR), using a FT-IR NICOLET 6700 (400–4000 cm^{-1}) spectrometer; (3) the absorption measurements (% Reflectance) were recorded with a Perkin Elmer Lambda 35 Spectrometer. As a reference, a certified reflectance standard has been used. During reflectance measurements, the reflected component of the sample beam was collected by the integrating sphere (Spectralon 50 mm Internal Diameter) and detected by the sphere detector. The sphere detector was a silicon photodiode while the detector signal represented the part of the sample beam that is not transmitted and not absorbed by the sample. The sample holder was 8° wedge and the used parameters were data interval, 1 nm; scan speed, 240 nm min^{-1} and slit, 1 nm; (4) X-ray diffraction with a Philips PW 1050 diffractometer with Bragg-Brentano geometry and Cu K_α radiation; the patterns have been scanned in steps of 0.02° (2θ) from 8° to 80° with a constant counting time of 30 s; (5) the scanning electron microscopy analysis were made by using a Quanta Inspect F microscope (FEI, the Netherland's) with field emission gun (FEG) having a 1.2 nm resolution, equipped with an energy-dispersive X-ray spectrometer (EDX) with a resolution at MnK of 133 eV. In what the sample preparation was concerned in the SEM-FEG (Scanning Electron Microscopy with Field Emission Gun) measurements, a small amount of powder was put onto a SEM aluminium sample holder on top of a carbon conductive tape; (6) for the transmission electron microscopy measurements, the bright field and high resolution images were obtained using a Tecnai™ G^2 F30 S-TWIN transmission electron microscope (FEI, the Nederland's), equipped with a STEM/HAADF detector, EDS (energy dispersive X-ray analysis) and EFTEM-EELS spectrometer (Electron Energy Loss Spectroscopy). The microscope operates at an acceleration voltage of 300 kV (Shottky field emitter) with a TEM point resolution of 2 Å and a TEM line resolution of 1.02 Å. The microscope was operated at an extraction voltage of 4500 V. The sample preparation was accomplished as follows: a small amount of powder was diluted into pure ethylic alcohol and left into an ultrasonic bath for approximately 15 min. After that, a small drop of the diluted solution was put onto a 400 mesh, holey carbon coated film Cu grid; (7) the specific surface area of the thermally treated zirconia powder has been measured by the Brunauer–Emmett–Teller (BET) method, using a Micromeritics ASAP 2020 apparatus. The sample has been outgassed in flowing N_2 at 300 °C for 2 h.

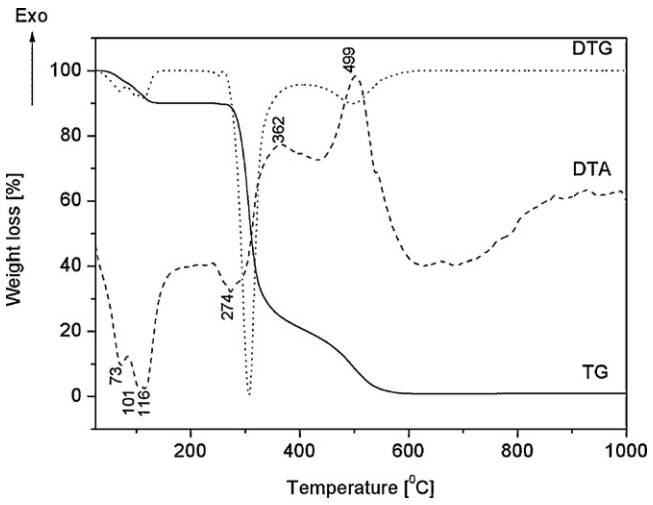

Fig. 1. Thermal behaviour of α-cyclodextrin.

3. Results and discussion

3.1. Thermal analysis

Once prepared, the zirconia powder containing α-cyclodextrin (ZrCD-untt sample) has been subjected to the characterization. In order to establish the thermal treatment which must be applied to remove the organic additive (for obtaining the ZrCD-tt sample) the characterization has begun with the thermal analysis.

The derivatograms of α-cyclodextrin and of the zirconia powders before (ZrCD-untt) and after thermal treatment (ZrCD-tt) are presented in Figs. 1–3.

The thermal behaviour of α-cyclodextrin (Fig. 1) has been fully described in a previous paper [40]. It evidences the following thermal effects: (a) two endothermic effects corresponding to 73 and 107 °C, respectively, due to water elimination; (b) one endothermic effect at 274 °C which is assigned to cyclodextrin decomposition; and finally (c) an exothermic effect at 499 °C, due to the cyclodextrin combustion.

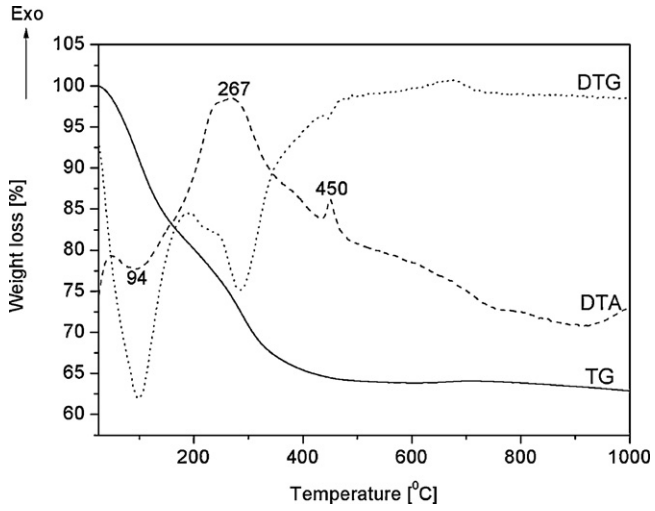

Fig. 2. Thermal behaviour of the untreated sample of ZrO_2 containing α-cyclodextrin (ZrCD-untt).

The thermal analysis of the sample ZrCD-untt (Fig. 2) which represents the as-synthesized sol–gel zirconia powder containing α-CD puts in evidence the influence of the ZrO_2 matrix on the thermal behaviour of the organic component. In its presence the temperature corresponding to the cyclodextrin combustion is significantly modified. Thus, α-CD is eliminated from the sample at much lower temperature (267 and 450 °C) compared to the temperature of combustion of the pure cyclodextrin which is around 499 °C. This observation is also valid in the case of sol–gel silica matrices [40] and could be considered as a proof of the fact that the cyclodextrin was included in the zirconia matrix. Based on the thermal behaviour study, the temperature of the thermal treatment has been chosen, in order to eliminate the organic molecules from the zirconia sample. After 20 h at 550 °C, the amorphous powder ZrCD-untt became a nanocrystalline one (ZrCD-tt), as XRD, SEM, and TEM analyses evidence. Its thermal behaviour is presented in Fig. 3.

It could be considered that a stable zirconia powder has been obtained. The thermogravimetric analysis curve (TGA) shows mass losses (of around 1% entirely) which are not coupled with thermal effects and could be assigned to dehydration of physically adsorbed water and desorption of chemically bound water (as OH^- groups), respectively [7,25]. Adamski et al. [18] consider the ZrO_2 formation

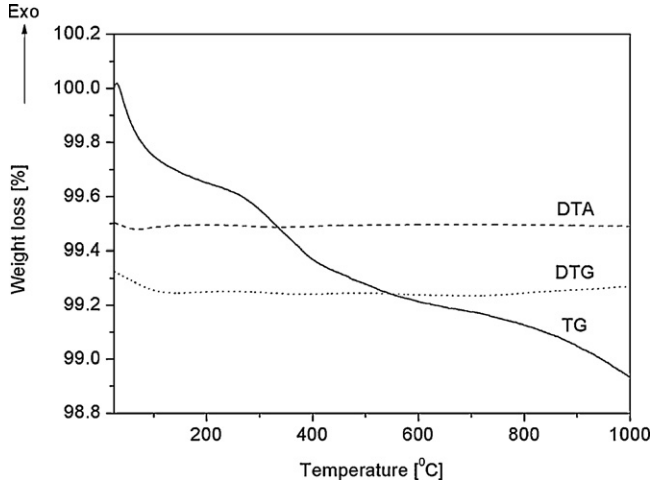

Fig. 3. Thermal behaviour of the thermally treated sample of ZrO_2 containing α-cyclodextrin (ZrCD-tt).

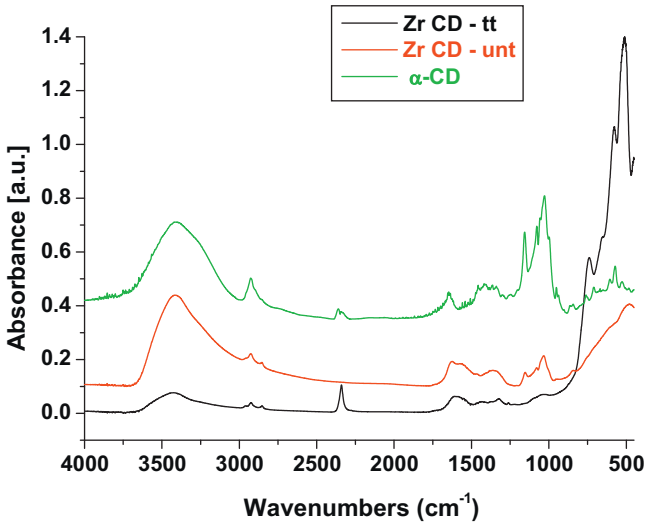

Fig. 4. IR spectra of both zirconia powders, before (ZrCD-untt) and after thermal treatment (ZrCD-tt), and of α-cyclodextrin.

as a quite complex process which includes several mutually related steps, such as dehydration. According to their results, the loosely bound water is released at temperatures below 170 °C, whereas the reticular one persists up to 450 °C. Such results show that the synthesis of our powder led to the incorporation of a certain amount of water into the framework of the gel, part of which (around 1%) still persists in the sample even after the thermal treatment. On the other hand, Rovira-Bru et al. [41] found on the TGA curve of the studied zirconia a total mass loss of about 0.42% in the domain of temperature from ~100 to ~960 °C. They assume that up to 350 °C the weight loss is due to loss of strongly hydrogen bound water, while surface hydroxyl condenses between 350 and 800 °C.

Comparing the TGA data of the amorphous zirconia powder and of the crystalline one, respectively, the difference between their mass losses can be observed. The first one is clearly larger than the second one, due to the fact that the amorphous material looses not only water, but also organic groups. This is in good agreement with the literature data [4,42].

It could be assumed that the effect of the organic additive (α-cyclodextrin) in the reaction mixture was similar to that of the different metal oxides (e.g. Y_2O_3, Ce_2O_3, MgO, CaO, etc.) generally used as dopants in order to stabilize the zirconia against phase transformation. This is in agreement with some literature data which suggest that organic additives can produce some desirable effects on the crystallite size and on the crystal phase of zirconia [16].

3.2. IR spectroscopy

In order to check the presence of the organic additive in the zirconia matrix, besides the thermal analysis, spectral methods (IR and UV–vis spectroscopy) have been used to characterize sample ZrCD-untt. Applying the mentioned methods to sample ZrCD-tt, the obtaining of a zirconia powder has been evidenced.

The results of the infrared spectroscopy investigations are presented in Fig. 4 and in Tables 1 and 2.

The measured wavelength values for α-cyclodextrin and ZrCD-tt sample have been presented in Tables 1 and 2 together with the literature data, for comparison. As it can be seen, in both cases the values overlap almost totally, which proves both the quality of the used organic additive and its elimination from the thermally treated zirconia powder. In the IR spectrum of the ZrCD-tt sample from Fig. 4, beside the wavelengths typical for ZrO_2 presented in

Table 1
IR bands frequencies for α-cyclodextrin according to our measurements and to the literature and the corresponding assignments.

Wavenumber in our sample (cm^{-1})	Wave number in literature (cm^{-1})	Assignment
3412	3412 [43]	OH stretching
2925	2925 [44]	CH stretching
2356	2361 [5,45,46]	CO_2 asymmetric stretch
1646	1646 [47,48]	Deformation mode of crystallization water present in the cyclodextrin cavity
1458, 1368 and 1336	1458 and 1368 [49]	CH deformation
1156	1156 [43]	CO stretching + OH bending
1087 and 1025	1087 and 1025 [50]	CO/CC stretching
755, 711, 608 and 572	755, 710 and 572 [51,52]	Pyranose ring vibration

Table 2, some peaks corresponding to water traces (1646 cm^{-1}), to CO_2 absorbed from the atmosphere (2337 cm^{-1}), and to CH stretching (2921 and 2852 cm^{-1}) which could belong to the residual α-cyclodextrin from the thermally treated sample are present. The quantity of these traces seems to be extremely low, since they are not found in the thermal analysis of the ZrCD-tt sample (Fig. 3).

In what the IR spectrum of the ZRCD-untt sample is concerned, the values of the determined wavelengths were: 3412, 2925, 2848, 1630, 1564, 1356, 1152, 1029, and 478 cm^{-1}, respectively. As it can be seen, these represent a combination of IR signals of both α-cyclodextrin and ZrO_2. Some of them are slightly shifted, proving the inclusion of the organic molecule in the ZrO_2 matrix.

So, it could be concluded that, as well as thermal analysis, the presented IR experimental data evidenced that the organic additive (α-cyclodextrin) was included by synthesis in the zirconia powder, from which it has been removed after the thermal treatment.

3.3. UV–vis spectroscopy

Typical UV–vis reflectance spectra for zirconia sample, before (ZrCD-untt) and after thermal treatment (ZrCD-tt) are presented in Fig. 5.

As it can be seen, there is a difference between the absorption peaks of the zirconia powder before the thermal treatment (sample ZrCD-untt) which contains the organic compound (α-CD), and the thermally treated sample (ZrCD-tt) from which the cyclodextrin has been eliminated. The presence of cyclodextrin in the sol–gel prepared zirconia powder is responsible for the appearance of the 13 nm batochromic shift of the absorption band, from 229 nm (in ZrCD-tt) to 216 nm (in ZrCD-untt). Also, it was observed that after thermal treatment, the reflectance is approximately two orders

Table 2
IR bands frequencies for ZrO_2 as it can be found in ZrCD-tt sample and in the literature and the corresponding assignments.

Wavenumber in sample named ZrCD-tt (cm^{-1})	Wavenumber for ZrO_2 in literature (cm^{-1})	Assignment
3428	3427 [53]	Zr—OH
–	764 [53]	Zr—O bending
–	800–200 [54]	ZrO_2
701 and 657	710 (745–490) [11,16]	Zr—O—Zr bond
580 and 514	734, 580 and 514 [55]	Zr—O vibration
514 and 440	734, 580, 514 and 440 [39,54,56,57]	Monoclinic ZrO_2
	480 [56]	Tetragonal ZrO_2

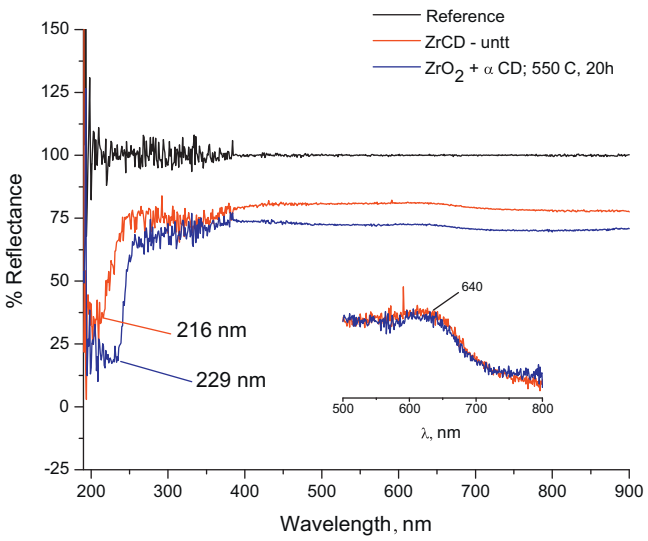

Fig. 5. UV–vis reflectance spectra of the prepared zirconia sample, before (ZrCD-untt) and after thermal treatment (ZrCD-tt) in comparison with the reference.

of magnitude smaller by comparison to that before the thermal treatment. Yu and Hu [22] reported the presence of the absorption peaks in the UV–vis spectra of zirconia prepared using organic surfactants as hexadecyltrimethyl ammonia bromide (C_{16}TMABr) and sodium dodecyl sulphate (SDS), at 200 and 210 nm, respectively.

In what the UV spectrum of ZrCD-tt sample is concerned, it evidences a higher absorption than that of the ZrCD-untt sample and it agrees well with those previously reported for zirconia. Chen et al. [58] give for zirconia an absorption peak at 230 nm, which is assigned to Zr—O—Zr linkage. For bulk phase ZrO_2, a band maximum in the UV–vis spectrum is also signalled between 230 and 240 nm, by Zaitseva and Gushikem [59]. According to López et al. [60] monoclinic phase of zirconia absorbs at lower energy (corresponding to 240 nm) than the tetragonal one (which absorbs around 200–210 nm). In line with Aita and Kwok [61] the band at 216 nm may be also corresponding to the interband transition in the monoclinic zirconium oxide. On the other hand, there are studies that indicate almost the same value of the absorption wavelength for both monoclinic and tetragonal zirconia phases that is 238, and 240 nm, respectively [62,63].

Apart from the main peaks of the zirconium presented spectra, a broad and weak peak can be observed in Fig. 5 at around 640 nm which could arise from transitions involving defect states or impurities [64].

It can be concluded that the UV–vis spectroscopy analysis has evidenced, once again, besides the thermal behaviour and the IR spectroscopy, the presence of the organic additive in the matrix of zirconia as a result of the synthesis process as well as its elimination, due to the proceeded thermal treatment.

3.4. X-ray diffraction

Being a typical structural characterization method, the XRD analysis has been applied to both zirconia powders: before (sample ZrCD-untt) and after thermal treatment (sample ZrCD-tt).

The results are presented in Fig. 6. It can be seen that the initial synthesized powder unthermally treated (ZrCD-untt) which contains α-cyclodextrin is amorphous. After the thermal treatment it becomes crystalline (ZrCD-tt).

From the view point of its composition, the zirconia powder resulted after the thermal treatment represents a mixture of two crystalline phases, the monoclinic one (M) which is predominant

Table 3
Structural factors calculated from the computerized profile analysis of the XRD spectra of the sample "ZrCD-tt" and of the zirconia standard (reference) "Ref." (according to the ASTM files 37–1484 and 42–1164) and the corresponding errors.

Identified phases		Structural factors[a]						
		a (Å)	b (Å)	c (Å)	β (°)	UCV (Å^3)	$\langle D\rangle$ (Å)	$\langle S\rangle \times 10^3$
Monoclinic (M)	Ref.	5.3129	5.2125	5.1471	99.218	140.70	–	–
	ZrCD-tt	5.2585(42)	5.1789(72)	5.1323(32)	99.26(18)	137.95(46)	388(10)	1.40(10)
Tetragonal (T)	Ref.	3.64	–	5.27	–	69.83	–	–
	ZrCD-tt	3.5488(97)	–	5.2253(183)	–	65.81(59)	214(15)	2.19(20)

[a] a, b, c, β – lattice parameters; UCV – unit cell volume; $\langle D\rangle$ – average crystallite size; $\langle S\rangle$ – average internal strain.

(91.4%) and the tetragonal (T) which is secondary (8.6%), confirming the literature data which assert a value of about 8% to the tetragonal phase for pHs 7–10 [34]. The relative amount of the monoclinic and tetragonal phases formed during calcination process has been determined based on Eq. (1) from the literature data [9,65–70].

$$x_m = \frac{I_m(1\,1\,1) + I_m(1\,1\,\bar{1})}{I_m(1\,1\,1) + I_m(1\,1\,\bar{1}) + I_t(1\,1\,1)} \quad (1)$$

where "I" represents the diffraction intensity of different lattice planes.

Table 3 presents the experimental data which have been obtained from computerized analysis of the XRD spectra with a proper X-RAY5.0 program that represents the upgrade form of the previous X-RAY3.0 program [71]. It also contains the corresponding calculated errors.

As it can be seen from Table 3, the values of the structural factors obtained from the crystalline powder ZrCD-tt are well correlated. The monoclinic phase presents a higher value of the average crystallite size than the tetragonal one, while the internal strains have the opposite behaviour, being smaller for the monoclinic symmetry than in the tetragonal case.

Comparing the structural factors values of the prepared zirconia powder ZrCD-tt with those of the reference (Ref.), it can be concluded that both elemental cells of the monoclinic phase and of the tetragonal one contract. Connecting this contraction with the high value of the internal strain of the T phase, important distortions in the lattice of our sample could be suggested.

XRD results proved that a nanocrystalline ZrO_2 powder has been prepared with average crystallite sizes of 38.8 nm (for the monoclinic phase), and 21.4 nm (for the tetragonal phase), respectively.

3.5. Electron microscopy

In order to complete the XRD characterization, electron microscopy has been used and correlations between both methods have been established, regarding the obtained crystalline zirconia nanopowder (ZrCD-tt).

3.5.1. Scanning electron microscopy (SEM)

SEM results for the ZrCD-tt sample are presented in Fig. 7. They confirm the literature data which assert that organic additives make particles assume spherical shape and reach fairly uniform size as well as prevent their agglomeration [16,22,69,72].

As it can be seen, equiaxial particles, uniform as shape and size, with a relatively reduced tendency of agglomeration can be observed. These observations are in good agreement with the literature data which indicate that a nanosized monoclinic zirconia powder from Degussa AG, Hanau presents a typical image of particles having sizes around 50 nm [73].

3.5.2. Transmission electron microscopy (TEM) and high resolution transmission electron microscopy (HRTEM) coupled with selected area electron diffraction (SAED)

In order to complete the SEM characterization of the thermally treated zirconia nanopowder, TEM, HRTEM and SAED analyses have been carried out. Fig. 8 presents the obtained results.

The TEM image of Fig. 8(a) allowed estimating an average particle size of 39.2 nm, in good agreement with the average crystallite size of 38.8 nm calculated from the XRD data (Table 3) for the monoclinic major phase and, thereby, proving the single crystal nature of the ZrO_2 particles.

The HRTEM image of Fig. 8(b) shows a particular porous morphology of the ZrO_2 particles obtained as a result of the organic

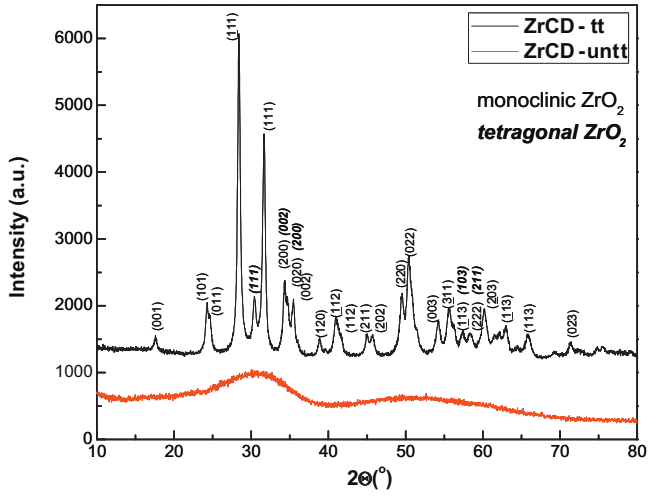

Fig. 6. XRD patterns of zirconia powder before (ZrCD-untt) and after thermal treatment (ZrCD-tt).

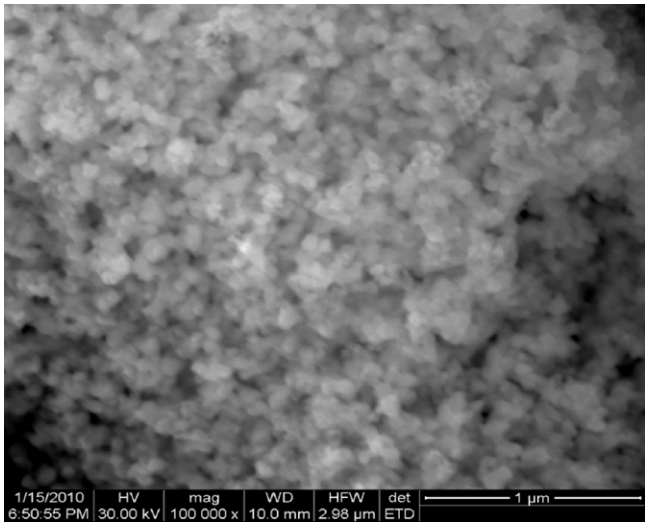

Fig. 7. SEM images of sample ZrCD-tt.

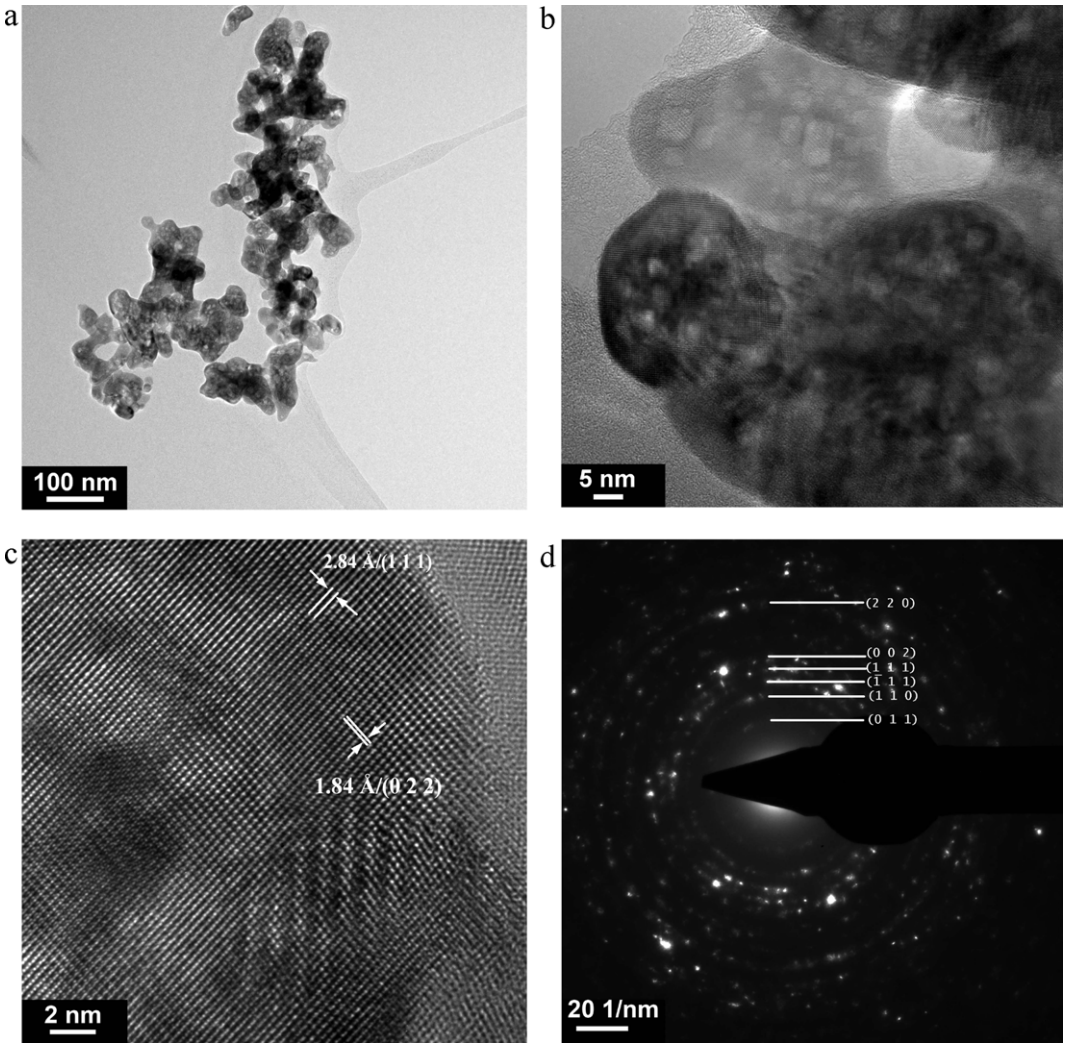

Fig. 8. TEM (a), HRTEM (b and c) and SAED (d) images of the ZrCD-tt sample.

compound (α-cyclodextrin) release during the thermal treatment. The light grey areas which are covered with consecutive lattice fringes suggest that the pores are closed and embedded within the grains. This hypothesis is also confirmed by the BET results which indicated a value of 19.11 $m^2\,g^{-1}$ for the specific surface area of the thermally treated ZrO_2 powder.

The higher magnification HRTEM image of Fig. 8(c) underlines the crystallinity of the ZrO_2 particles, showing well resolved and equidistant lattice fringes. These fringes are separated by 2.84 Å and 1.84 Å, respectively, which agrees well with the interplanar spacing corresponding to the (1 1 1) and (0 2 2) planes of monoclinic zirconia.

The high crystallinity degree of the ZrCD-tt nanopowder was also confirmed by the well-marked, bright spots forming the concentric rings which correspond to the SAED patterns of monoclinic ZrO_2 (Fig. 8(d)).

The mean particle size of the ZrCD-tt powder was calculated using the OriginPro 8.5 software (statistics on column) by taking into account approximately 500 non-agglomerated particles (from images obtained from various microscopic fields), whose diameter was accurately measured using the microscope software DigitalMicrograph 1.8.0. The histogram describing the particle size distribution based on these measurements is presented in Fig. 9.

Particles between 32 and 50 nm respectively have been detected. The mean size particle was of 39.18 nm, in a very good agreement with the estimated value (39.20 nm) from the TEM image of Fig. 8(a).

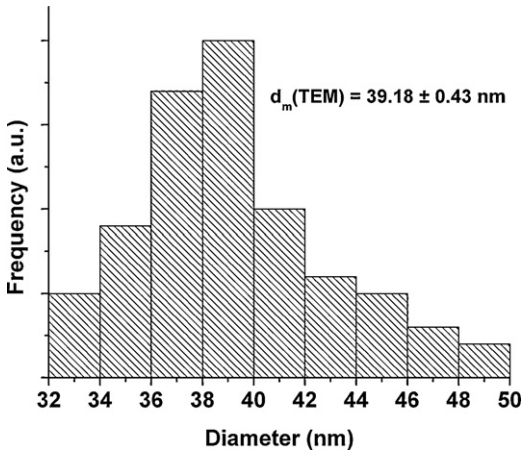

Fig. 9. Particle size distribution obtained by means of TEM measurements performed on ~500 non-agglomerated particles taken from various microscopic fields.

4. Conclusions

The sol–gel synthesis of a zirconia nanopowder has been performed, in the presence of α-cyclodextrin as organic additive. The inclusion of the oligosaccharide in the zirconia matrix has been evidenced.

The crystalline nanopowder resulted after thermal treatment (sample ZrCD-tt), consisted of a mixture of monoclinic (predominant: 91.4%) and tetragonal (8.6%) zirconia phases. The organic additive seems to produce some desirable effects on the crystallite size and on the crystal phase of zirconia, ensuring its stability against the phase transformation.

The α-cyclodextrin has influenced the powder properties by making the particles to assume spherical shape and reach fairly uniform size as well as preventing their agglomeration. Furthermore, the organic additive led to a certain porous morphology of the zirconia particles that is the pores are embedded within the grains.

In conclusion, using only the sol–gel method, in the experimental conditions mentioned before, at room temperature and in the presence of α-cyclodextrin (a non-toxic and available organic compound) it was possible to obtain a stable, nanocrystalline zirconia powder with a special porous morphology which allows its application in the thermal barrier coatings domain.

Acknowledgements

This work has been performed in the frame of 7.2 theme of the Romanian Academy programme: oxide systems obtained by the sol–gel method (2011).

References

[1] V. Ramaswamy, M. Bhawat, D. Srinivas, A.V. Ramaswamy, Catal. Today 97 (2004) 63–70.
[2] P. Moravec, J. Smolík, H. Heskinen, J.M. Mäkelä, V.V. Levdansky, Aerosol Air Qual. Res. 7 (2007) 563–577.
[3] A.P. Naumenko, N.I. Berezovska, M.M. Biliy, O.V. Shevchenko, Phys. Chem. Solid State 9 (2008) 121–125.
[4] B.L. Kirsch, S.H. Tolbert, Adv. Funct. Mater. 13 (2003) 281–288.
[5] L.E. Davies, N.A. Bonini, S. Locatelli, E.E. Gonzo, Latin Am. Appl. Res. 35 (2005) 23–28.
[6] J. Widoniak, S. Eiden-Assmann, G. Maret, Eur. J. Inorg. Chem. (2005) 3149–3155.
[7] J.P. Marković, S.K. Milonjić, J. Serb. Chem. Soc. 71 (2006) 613–619.
[8] I.-K. Jun, Y.-H. Koh, J.-H. Song, H.-E. Kim, J. Am. Ceram. Soc. 89 (2006) 2021–2026.
[9] A. Adamski, P. Jakubus, Z. Sojka, Mater. Sci. Poland 26 (2008) 373–380.
[10] G. Duan, C. Zhang, A. Li, X. Yang, L. Lu, X. Wang, Nanoscale Res. Lett. 3 (2008) 118–122.
[11] S. Nagarajan, N. Rajendran, J. Sol–Gel Sci. Technol. 52 (2009) 188–196.
[12] X.H. Jia, J.J. Yang, Y.M. Zuo, Chinese Chem. Lett. 12 (2001) 439–442.
[13] K. Joy, S. Lakshmy, P.B. Nair, G.P. Daniel, J. Alloys Compd. 512 (2012) 149–155.
[14] G. Dercz, K. Prusik, L. Pajak, JAMME 18 (2006) 259–262.
[15] H.A. Abbas, F.F. Hamad, A.K. Mohamad, Z.M. Hanafi, M. Kilo, Diffus. Fundam. 8 (2008) 7.1–7.8.
[16] F. Heshmatpour, R.B. Aghakhanpour, Powder Technol. 205 (2011) 193–200.
[17] J.-C. Yu, S.-W. Hu, Chinese J. Struct. Chem. 25 (2006) 1512–1516.
[18] A. Adamski, P. Jakubus, Z. Sojka, Nukleonika 51 (2006) S27–S33.
[19] Y. Kan, S. Li, P. Wang, G.-J. Zhang, O. Van der Biest, J. Vleugels, Solid State Ionics 179 (2008) 1531–1534.
[20] Y.-W. Hsu, K.-H. Yang, K.-M. Chang, S.-W. Yeh, M.-C. Wang, J. Alloys Compd. 509 (2011) 6864–6870.
[21] P.M. Abdala, D.G. Lamas, M.C.A. Fantini, A.F. Craievich, J. Alloys Compd. 495 (2010) 561–564.
[22] J.-C. Yu, S.-W. Hu, Chinese J. Struct. Chem. 24 (2005) 1133–1139.
[23] C. Suciu, L. Gagea, A.C. Hoffmann, M. Mocean, Chem. Eng. Sci. 61 (2006) 7831–7835.
[24] V.G. Zavodinski, A.N. Chibisov, J. Phys. Conf. Ser. 29 (2006) 173–176.
[25] M. Rezaei, S.M. Alavi, S. Sahebdelfar, L. Xinmei, Z.F. Yan, J. Mater. Sci. 42 (2007) 7086–7092.
[26] Q. Chang, J.-E. Zhou, Y. Wang, G. Meng, Adv. Powder Technol. 20 (2009) 371–374.
[27] F. Prete, A. Rizzuti, L. Esposito, A. Tucci, C. Leonelli, J. Am. Ceram. Soc. 94 (2011) 3587–3590.
[28] C.J. Reidy, T.J. Fleming, S. Hampshire, M.R. Towler, Int. J. Appl. Ceram. Technol. 8 (2011) 1475–1485.
[29] R. Pazhani, H.P. Kumar, A. Varghese, A.M.E. Raj, S. Solomon, J.K. Thomas, J. Alloys Compd. 509 (2011) 6819–6823.
[30] X. Bokhimi, A. Morales, O. Novaro, M. Portilla, T. López, F. Tzompantzi, R. Gómez, J. Solid State Chem. 135 (1998) 28–35.
[31] S.-G. Chen, Y.-S. Yin, D.-P. Wang, J. Mol. Struct. 690 (2004) 181–187.
[32] O. Van Cantfort, B. Michaux, R. Pirard, J.P. Pirard, J. Sol–Gel Sci. Technol. 8 (1997) 207–211.
[33] C. Stöcker, A. Baiker, J. Sol–Gel Sci. Technol. 10 (1997) 269–282.
[34] G. Fetter, P. Bosch, T. López, J. Sol–Gel Sci. Technol. 23 (2002) 199–203.
[35] L.F. Liotta, G. Pantaleo, A. Macaluso, G. Marcì, S. Gialanella, G. Deganello, J. Sol–Gel Sci. Technol. 28 (2003) 119–132.
[36] T. Rivera, J. Azorín, M. Barrera, A.M. Soto, R. Sosa, C. Furetta, Radiat. Eff. Defect Solid 162 (2007) 597–603.
[37] A. Taavoni-Gilan, E. Taheri-Nassaj, R. Naghizadeh, H. Akhondi, Ceram. Int. 36 (2010) 1147–1153.
[38] S. Salehi, M.H. Fathi, Ceram. Int. 36 (2010) 1659–1667.
[39] J. Ortiz-Landeros, M.E. Contreras-Garciá, H. Pfeiffer, Adv. Technol. Mater. Mater. Proc. J. 9 (2007) 119–124.
[40] M. Raileanu, L. Todan, M. Crisan, A. Braileanu, A. Rusu, C. Bradu, A. Carpov, M. Zaharescu, J. Environ. Prot. 1 (2010) 302–313.
[41] M. Rovira-Bru, F. Giralt, Y. Cohen, J. Colloid Interface Sci. 235 (2001) 70–79.
[42] M.J. Bockmeyer, R. Krüger, J. Am. Ceram. Soc. 91 (2008) 1070–1076.
[43] D. Bongiorno, L. Ceraulo, M. Ferrugia, F. Filizzola, A. Ruggirello, V.T. Liveri, ARKIVOC xiv (2005) 118–130.
[44] F.B. De Sousa, J.D.T. Guerreiro, M. Ma, D.G. Anderson, C.L. Drun, R.D. Sinisterra, R. Langer, J. Mater. Chem. 20 (2010) 9910–9917.
[45] M. Avram, Gh.D. Mateescu, Spectroscopia în infraroşu. Aplicaţii în chimia organic, Editura Tehnică Bucureşti, 1966, p. 55.
[46] E. Schmidt, N. Aslesen, J. Phys. Chem. Lab. 9 (2005) 54–63.
[47] J.C. Netto-Ferreira, V. Wintgens, L.F. Vieira Ferreira, A.R. Garcia, L.M. Ilharco, M.J. Lemos, J. Photochem. Photobiol. A: Chem. 132 (2000) 209–217.
[48] J.M. Gavira, A. Hernanz, I. Bratu, Vib. Spectrosc. 32 (2003) 137–146.
[49] G. Balş, G.M. Simu, J. Eng. Ann. Fac. Eng. Hunedoara VII (2009) 107–109.
[50] T. Uyar, F. Besenbacher, Eur. Polym. J. 45 (2009) 1032–1037.
[51] S. Jaiswal, B. Duffy, A.K. Jaiswal, N. Stobie, P. McHale, Int. J. Antimicrob. Agents 36 (2010) 280–283.
[52] I. Bratu, S. Astilean, C. Ionesc, E. Indrea, J.P. Huvenne, P. Legrand, Spectrochim. Acta Part A 54 (1998) 191–196.
[53] H. Wang, P. Xu, W. Zhong, L. Shen, Q. Du, Polym. Degrad. Stabil. 87 (2005) 319–327.
[54] M. Zhang, E.K.H. Salje, A.H. Wang, X.J. Li, C.S. Xie, S.A.T. Redfern, R.X. Li, J. Phys.: Condens. Matter 17 (2005) 6363–6376.
[55] A. Agraval, Effect of nickel concentration on stabilization of tetragonal zirconia, Thesis for Bachelor of Technology in Ceramic Engineering, Department of Ceramic Engineering National Institute of Technology Rourkela, 2009.
[56] F. del Monte, W. Larsen, J.D. Mackenzie, J. Am. Ceram. Soc. 83 (2000) 628–634.
[57] H.C. Zeng, S. Shi, J. Non-Cryst. Solids 185 (1995) 31–40.
[58] X.-R. Chen, Y.-H. Ju, C.-Y. Mou, J. Phys. Chem. C 111 (2007) 18731–18737.
[59] G. Zaitseva, Y. Gushikem, J. Brazil Chem. Soc. 13 (2002) 611–617.
[60] E.F. López, V.S. Escribano, M. Panizza, M.M. Carnasciali, G. Busca, J. Mater. Chem. 11 (2001) 1891–1897.
[61] C.R. Aita, H.K. Kwok, J. Am. Ceram. Soc. 73 (1990) 3209–3214.
[62] H.R. Sahu, G.R. Rao, Bull. Mater. Sci. 23 (2000) 349–354.
[63] G.R. Rao, H.R. Sahu, Proc. Indian Acad. Sci. (Chem. Sci.) 113 (2001) 651–658.
[64] L. Kumari, G.H. Du, W.Z. Li, R. Selva Vennila, S.K. Saxena, D.Z. Wang, Ceram. Int. 35 (2009) 2401–2408.
[65] J. Matta, J.-F. Lamonier, E. Abi-Aad, E.A. Zhilinskaya, A. Aboukais, Phys. Chem. Chem. Phys. 1 (1999) 4975–4980.
[66] J. Moon, H. Choi, C. Lee, J. Ceram. Process. Res. 1 (2000) 69–73.
[67] J. Tang, F. Zhang, P. Zoogman, J. Fabbri, S.-W. Chan, Y. Zhu, L.E. Brus, M.L. Steigerwald, Adv. Funct. Mater. 15 (2005) 1595–1602.
[68] S. Shukla, S. Seal, Rev. Adv. Mater. Sci. 4 (2003) 123–126.
[69] G.-H. Li, Z.-L. Hong, H. Yang, Chinese J. Struct. Chem. 27 (2008) 498–502.
[70] W. Pabst, J. Havrda, E. Gregorová, B. Krčmová, Ceram. Silikáty 44 (2000) 41–47.
[71] N. Drăgan, D. Crişan, C. Lepădatu, Rom. J. Mater. 33 (2003) 133–148.
[72] L. Zhou, J. Xu, X. Li, F. Wang, Mater. Chem. Phys. 97 (2006) 137–142.
[73] C. Oetzel, R. Clasen, J. Mater. Sci. 41 (2006) 8130–8137.